Anal. Chem. **2009,** *81,* 10149–10155

Bipolar Electrode Focusing: The Effect of Current and Electric Field on Concentration Enrichment

Robbyn K. Perdue,[†] Derek R. Laws,[†] Dzmitry Hlushkou,[‡] Ulrich Tallarek,*[,‡] and Richard M. Crooks*[,†]

Department of Chemistry and Biochemistry, Center for Electrochemistry, and the Center for Nano- and Molecular Science and Technology, The University of Texas at Austin, 1 University Station, A5300, Austin, Texas 78712-0165, and Department of Chemistry, Philipps-Universität Marburg, Hans-Meerwein-Strasse, 35032 Marburg, Germany

Bipolar electrode focusing at discontinuous bipolar electrodes (BPEs) provides new insight into the faradaic current and electric field characteristics associated with the technique and allows for the controlled transport of a focused anionic tracer in a microfluidic channel. The findings corroborate our previously reported simulation results, which describe the formation of an extended electric field gradient leading to concentration enrichment. This gradient has been attributed to the passage of faradaic current through a BPE affixed to the floor of the microchannel. Our results demonstrate that the onset of faradaic current is coincident with the onset of concentration enrichment. Utilizing an array of microband electrodes, the tracer may be passed from one stationary position to another by rapidly relocating the BPE. However, the tracer movement is limited to one direction, confirming that the electrophoretic velocity of the analyte exceeds the electroosmosis-driven bulk fluid flow velocity at only the cathodic edge of the BPE.

In this paper, we demonstrate concentration enrichment of an anionic tracer using discontinuous bipolar electrodes (BPEs) (Figure 1). The key finding is that these microband electrodes can be configured to induce analyte concentration[1−3] but with some significant advantages compared to our previous reports that employed a single, continuous BPE design. Specifically, any two microband electrodes in a microchannel may be connected externally to yield a BPE.[4,5] This makes it possible to simultaneously measure the current flowing through a BPE and the corresponding effect on the redistribution of the tracer in the microchannel. This correlation provides valuable insights into the role of faradaic reactions in the formation of electric field gradients and the onset of concentration enrichment. Additionally, arrays of microbands may be used to measure the electric field strength in solution at different locations in a microchannel. This provides a direct probe of the electric field and can, therefore, corroborate results obtained by numerical simulation. Finally, the accessibility of multiple BPE configurations within a microband array provides a means for controlled, unidirectional transport of the concentrated tracer.

Lab-on-a-chip devices are at the forefront of development of clinical diagnostic tools due to their ability to carry out rapid, integrated sample processing. In these devices, microfluidic channels allow transport and processing of nano- to microliter-scale samples. This attribute can be particularly advantageous in biomedical diagnostic applications in which sample volumes are often small. However, such small sample volumes, coupled with low analyte concentrations, lead to limited numbers of molecules being available for detection. Accordingly, ex-situ processing steps are frequently required to provide a more concentrated sample for chip-based analyses. However, for many applications, integration of a simple concentration enrichment module onto a lab-on-a-chip device is preferable to off-chip processing. This is the issue addressed here.

The majority of concentration enrichment methods presently used on microchips were originally developed for capillary electrophoresis. Many of these techniques rely on manipulation of the electrokinetic motion of an analyte. Some of the most well-known of these are field-amplified sample stacking,[6,7] isotachophoresis,[8−12] electric field gradient focusing (EFGF),[13−16] and

* To whom correspondence should be addressed. E-mail: crooks@cm.utexas.edu (R.M.C.); tallarek@staff.uni-marburg.de (U.T.).

[†] The University of Texas at Austin.

[‡] Philipps-Universität Marburg.

(1) Dhopeshwarkar, R.; Hlushkou, D.; Nguyen, M.; Tallarek, U.; Crooks, R. M. *J. Am. Chem. Soc.* **2008**, *130*, 10480–10481.

(2) Hlushkou, D.; Perdue, R. K.; Dhopeshwarkar, R.; Crooks, R. M.; Tallarek, U. *Lab Chip* **2009**, *9*, 1903–1913.

(3) Laws, D. R.; Hlushkou, D.; Perdue, R. K.; Tallarek, U.; Crooks, R. M. *Anal. Chem.*, **2009**, *81*, 8923−8929.

(4) Ordeig, O.; Godino, N.; del Campo, J.; Munoz, F. X.; Nikolajeff, F.; Nyholm, L. *Anal. Chem.* **2008**, *80*, 3622–3632.

(5) Arora, A.; Eijkel, J. C. T.; Morf, W. E.; Manz, A. *Anal. Chem.* **2001**, *73*, 5633–5633.

(6) Chien, R. L. *Electrophoresis* **2003**, *24*, 486–497.

(7) Lichtenberg, J.; Verpoorte, E.; de Rooij, N. F. *Electrophoresis* **2001**, *22*, 258–271.

(8) Chen, L.; Prest, J. E.; Fielden, P. R.; Goddard, N. J.; Manz, A.; Day, P. J. R. *Lab Chip* **2006**, *6*, 474–487.

(9) Gebauer, P.; Thormann, W.; Bocek, P. *J. Chromatogr., A* **1992**, *608*, 47–57.

(10) Jung, B.; Bharadwaj, R.; Santiago, J. G. *Anal. Chem.* **2006**, *78*, 2319–2327.

(11) Kohlheyer, D.; Eijkel, J. C. T.; van den Berg, A.; Schasfoort, R. B. M. *Electrophoresis* **2008**, *29*, 977–993.

(12) Xu, Z. Q.; Nishine, T.; Arai, A.; Hirokawa, T. *Electrophoresis* **2004**, *25*, 3875–3881.

(13) Kelly, R. T.; Li, Y.; Woolley, A. T. *Anal. Chem.* **2006**, *78*, 2565–2570.

(14) Liu, J.; Sun, X.; Farnsworth, P. B.; Lee, M. L. *Anal. Chem.* **2006**, *78*, 4654–4662.

(15) Petsev, D. N.; Lopez, G. P.; Ivory, C. F.; Sibbet, S. S. *Lab Chip* **2005**, *5*, 587–597.

(16) Warnick, K. F.; Francom, S. J.; Humble, P. H.; Kelly, R. T.; Woolley, A. T.; Lee, M. L.; Tolley, H. D. *Electrophoresis* **2005**, *26*, 405–414.

10.1021/ac901913r CCC: $40.75
Published on Web 11/18/2009

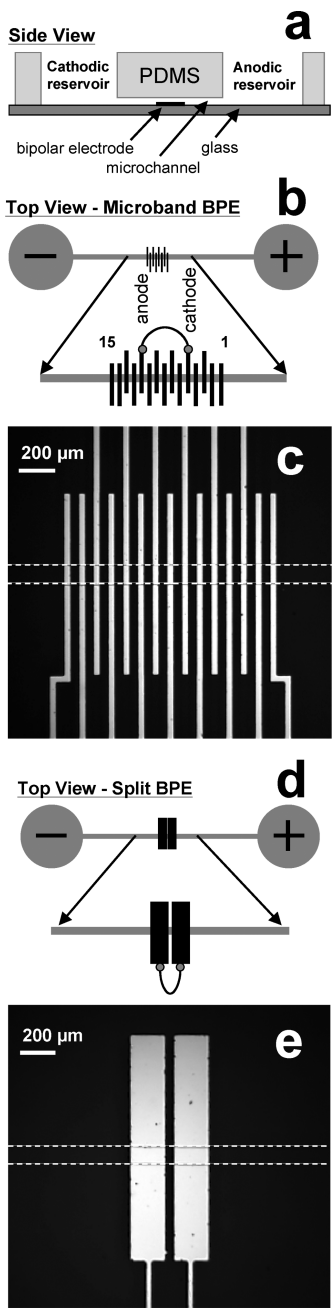

Figure 1. (a) Microfluidic device used in the experiments reported here. The PDMS microchannel measures 6.0 mm × 100 μm × ~20 μm with 4.0 mm diameter reservoirs. The PDMS channel is sealed to a glass slide with the gold BPE microfabricated at its center. (b) Top view schematic of the microfluidic channel showing detail of a microband array with a jumper wire connecting electrodes 5 and 11 to create a BPE. (c) An optical micrograph of the gold microband array (40 μm lines and spaces). (d) Top view schematic of the microfluidic channel showing a split BPE with a jumper wire connecting the two sides. (e) Optical micrograph of a gold split bipolar electrode. The electrode is 500 μm long with a 50 μm gap in the center. The dashed white lines in (c) and (e) indicate the location of the microchannel.

isoelectric focusing (IEF).[17−21] Some newer techniques that were specifically designed for microchip applications include concentration enrichment by electrostatic exclusion at nanochannels and nanoporous membranes[22−36] and temperature gradient focusing (TGF) within microchannels.[37−40] Techniques such as IEF, EFGF, and TGF have the added advantage of focusing individual analytes at particular locations along a gradient. Indeed, opposing forces may act to counter diffusional band broadening, therefore allowing enhanced enrichment and simultaneous high-resolution separations.[3]

The most widely used focusing technique is IEF due to its applicability to protein separations. IEF employs a pH gradient to focus each analyte at a specific location based on its isoelectric point (pI). The major limitations of IEF are the necessity to generate a high-quality static pH gradient and the fact that proteins have low solubility in their net-neutral state (where pH = pI).[41] The appeal of newly developed techniques, such as TGF and EFGF, is that charged (and hence more soluble) analytes can be enriched 1000- to 10 000-fold.[41] One EFGF technique called dynamic field gradient focusing (DFGF) utilizes an array of electrodes to directly control the shape of the electric field.[42]

We recently reported electrokinetic focusing of anions in a microchannel using a BPE to control the local electric field.[1,2] The BPE is a conductive material that is not connected to an external power supply, and therefore, it is free to float to an equilibrium potential. If there is a sufficient potential dropped across the solution above a BPE, it can act as an electrode at which cathodic and anodic reactions occur simultaneously at opposite ends. By providing a low resistance path for the passage of current, the BPE results in less ionic current being carried by the solution above the electrode. Therefore, the electric field in the vicinity of

(17) Cui, H.; Horiuchi, K.; Dutta, P.; Ivory, C. F. *Anal. Chem.* **2005**, *77*, 1303–1309.
(18) Dauriac, V.; Descroix, S.; Chen, Y.; Peltre, G.; Sénéchal, H. *Electrophoresis* **2008**, *29*, 2945–2952.
(19) Herr, A. E.; Molho, J. I.; Drouvalakis, K. A.; Mikkelsen, J. C.; Utz, P. J.; Santiago, J. G.; Kenny, T. W. *Anal. Chem.* **2003**, *75*, 1180–1187.
(20) Li, C.; Yang, Y.; Craighead, H. G.; Lee, K. H. *Electrophoresis* **2005**, *26*, 1800–1806.
(21) Yao, B.; Yang, H.; Liang, Q.; Luo, G.; Wang, L.; Ren, K.; Gao, Y.; Wang, Y.; Qiu, Y. *Anal. Chem.* **2006**, *78*, 5845–5850.
(22) Cannon, D. M., Jr.; Kuo, T.-C.; Bohn, P. W.; Sweedler, J. V. *Anal. Chem.* **2003**, *75*, 2224–2230.
(23) Dhopeshwarkar, R.; Sun, L.; Crooks, R. M. *Lab Chip* **2005**, *5*, 1148–1154.
(24) Foote, R. S.; Khandurina, J.; Jacobson, S. C.; Ramsey, J. M. *Anal. Chem.* **2005**, *77*, 57–63.
(25) Gatimu, E. N.; King, T. L.; Sweedler, J. V.; Bohn, P. W. *Biomicrofluidics* **2007**, *1*, 021502.
(26) Han, J.; Fu, J.; Schoch, R. B. *Lab Chip* **2008**, *8*, 23–33.
(27) Hlushkou, D.; Dhopeshwarkar, R.; Crooks, R. M.; Tallarek, U. *Lab Chip* **2008**, *8*, 1153–1162.
(28) Jin, X.; Joseph, S.; Gatimu, E. N.; Bohn, P. W.; Aluru, N. R. *Langmuir* **2007**, *23*, 13209–13222.
(29) Khandurina, J.; Jacobson, S. C.; Waters, L. C.; Foote, R. S.; Ramsey, J. M. *Anal. Chem.* **1999**, *71*, 1815–1819.
(30) Kim, S. M.; Burns, M. A.; Hasselbrink, E. F. *Anal. Chem.* **2006**, *78*, 4779–4785.
(31) Kim, T.; Meyhöfer, E. *Anal. Chem.* **2008**, *80*, 5383–5390.
(32) Piruska, A.; Branagan, S.; Cropek, D. M.; Sweedler, J. V.; Bohn, P. W. *Lab Chip* **2008**, *8*, 1625–1631.
(33) Song, S.; Singh, A. K.; Kirby, B. J. *Anal. Chem.* **2004**, *76*, 4589–4592.
(34) Wang, Y.-C.; Stevens, A. L.; Han, J. *Anal. Chem.* **2005**, *77*, 4293–4299.
(35) Zhang, Y.; Timperman, A. T. *Analyst* **2003**, *128*, 537–542.
(36) Zhou, K.; Kovarik, M. L.; Jacobson, S. C. *J. Am. Chem. Soc.* **2008**, *130*, 8614–8616.
(37) Balss, K. M.; Vreeland, W. N.; Phinney, K. W.; Ross, D. *Anal. Chem.* **2004**, *76*, 7243–7249.
(38) Hoebel, S. J.; Balss, K. M.; Jones, B. J.; Malliaris, C. D.; Munson, M. S.; Vreeland, W. N.; Ross, D. *Anal. Chem.* **2006**, *78*, 7186–7190.
(39) Kim, S. M.; Sommer, G. J.; Burns, M. A.; Hasselbrink, E. F. *Anal. Chem.* **2006**, *78*, 8028–8035.
(40) Ross, D.; Locascio, L. E. *Anal. Chem.* **2002**, *74*, 2556–2564.
(41) Song, S.; Singh, A. *Anal. Bioanal. Chem.* **2006**, *384*, 41–43.
(42) Huang, Z.; Ivory, C. F. *Anal. Chem.* **1999**, *71*, 1628–1632.

the electrode is suppressed. The diversion of current through the BPE is termed faradaic depolarization.[43] The ratio of the current passing through the BPE (i_{BPE}) to the total current passing through the fluidic channel (i_{tot}) defines the degree of depolarization.

As discussed in detail later, the faradaic reactions taking place at the BPE lead to the formation of an extended electric field gradient that can be used for concentration enrichment. During enrichment, anions entering the channel from the anodic reservoir via cathodic electroosmotic flow (EOF) encounter an increasing electric field that eventually becomes strong enough to exactly counteract the EOF. Accordingly, anions focus at a unique position where the electrophoretic and electroosmotic velocities of the analyte sum to zero. We call this phenomenon bipolar electrode focusing, and it has the advantage of being applicable to all anionic analytes under the appropriate conditions. It is also a simple technique that is capable of simultaneously concentrating and separating analytes.[3]

Here, experimental results and interpretive simulations are presented that provide new fundamental and applied insights into bipolar electrode focusing. Specifically, discontinuous BPEs replace the continuous BPEs used in our previous reports.[1−3] This advance makes it possible to directly correlate the extent of concentration enrichment to in situ amperometric and potentiometric measurements. The results of these studies indicate that concentration enrichment is coincident with the onset of faradaic electrochemistry at the BPE. Moreover, by measuring the potential between neighboring microband electrodes, it is possible to map the intrachannel electric field gradient and compare it to results derived from numerical simulations. Finally, the use of discontinuous microband electrodes makes it possible to control transport of a focused analyte band. This observation is potentially important, because it may provide a means to isolate a concentrated analyte band from a crude sample and then move it to a desired location for further processing without the need for additional channels or complex pressure switching.

EXPERIMENTAL SECTION

Chemicals. BODIPY disulfonate ($BODIPY^{2-}$, Molecular Probes, Eugene, OR) was used as a fluorescent tracer to quantitate the degree of concentration enrichment. Molecular biology grade 1.0 M TRIS−HCl buffer (Fisher Biotech, Fair Lawn, NJ) was diluted to 5.0 mM (pH 8.0) with deionized water (18.0 MΩ·cm, Milli-Q Gradient System, Millipore) and used as background electrolyte in all experiments. The silicone elastomer and curing agent (Sylgard 184) used to prepare the poly(dimethylsiloxane) (PDMS) microfluidic devices were obtained from K. R. Anderson, Inc. (Morgan Hill, CA).

Device Fabrication. The hybrid PDMS/glass microfluidic devices and gold electrodes were prepared by a previously published procedure.[44] Briefly, a microfluidic channel (6.0 mm long, 100 μm wide, and ~20 μm high) spanning two 4.0 mm diameter reservoirs was fabricated from PDMS. Next, 100 nm thick gold electrodes (no adhesion layer, Evaporated Metal Films, Ithaca, NY) were microfabricated on glass slides by standard photolithographic techniques. Finally, the PDMS and glass were exposed to an O_2 plasma (60 W, model PDC-32G, Harrick Scientific, Ossining, NY) for 15 s and then bonded together. The microband electrodes were positioned at the center of the channel and protruded from beneath the PDMS monolith so they could be interconnected via an external jumper wire.

Three distinct new electrode designs were used in these experiments (Figure 1). The split BPE (Figure 1d,e) is most similar to the 500 μm long continuous BPEs used in our previous studies.[1−3] The outer edges of the split BPE are separated by 500 μm and there is a 50 μm gap at its center. The total electrode area exposed to the solution is 4.5×10^{-4} cm^2. This design was used to determine the current passing through the BPE. The second type of BPE is an array of 15 gold microband electrodes consisting of 40 μm lines and spaces (Figure 1b,c). Current measurements at a pair of these microbands, which have an outer edge-to-edge distance of 520 μm and a total exposed area of 0.8×10^{-4} cm^2, were compared with those obtained using the split BPE to confirm that the current in the microbands (and the corresponding effect on the electric field) is not significantly affected by the smaller exposed electrode area. This design was also used for all electric field profiling measurements. The third design consists of 15 microbands, but in this case, the electrodes are 20 μm wide and the spaces between electrodes are 80 μm. This design was used solely for analyte transport experiments in which the wider gaps between electrodes provided a clearer view of the focused analyte movement.

Concentration Enrichment Experiments. Prior to each experiment, the microfluidic channel was rinsed by introducing 40.0 μL of 5.0 mM TRIS buffer (pH 8.0) into the anodic reservoir and 15.0 μL into the cathodic reservoir. The buffer solution was allowed to flow through the microchannel for 20 min in response to the solution height differential (~2 mm). Next, the rinsing solution in each of the reservoirs was replaced with 40.0 μL of 0.1 μM $BODIPY^{2-}$ in 5.0 mM TRIS. Additional microliter increments of the same solution were added to each reservoir in individual experiments as indicated in the Results and Discussion section.

Concentration enrichment experiments were carried out as follows. First, two microband electrodes having the desired separation were connected via a conductive wire. Second, a driving voltage (E_{tot} = 35.0 V) was applied across the microchannel using a high-voltage power supply (LLS9120, TDK-Lambda Americas, Inc., San Diego, CA) connected to the microfabricated gold driving electrodes spanning the bottoms of the reservoirs. Finally, the extent of enrichment was determined by fluorescence microscopy.

Fluorescence Measurements. Enrichment of the $BODIPY^{2-}$ tracer dye was monitored using a fluorescence microscope (Multizoom AZ100, Nikon, Japan) fitted with a CCD camera (QuantEM 512SC, Photometrics, Tucson, AZ). An inverted epifluorescence microscope (Eclipse TE 2000-U, Nikon) fitted with a CCD camera (Cascade 512B, Photometrics) was only used to obtain images during controlled analyte transport experiments. Values of the enrichment factor were determined by comparing the region of maximum intensity in the concentrated band of dye to calibrated fluorescence intensities. All measurements were corrected for the background intensity.

(43) Duval, J.; Kleijn, J. M.; van Leeuwen, H. P. *J. Electroanal. Chem.* **2001**, *505*, 1–11.
(44) McDonald, J. C.; Duffy, D. C.; Anderson, J. R.; Chiu, D. T.; Wu, H.; Schueller, O. J. A.; Whitesides, G. M. *Electrophoresis* **2000**, *21*, 27–40.

Current Measurements. Current flowing through the BPEs was measured by connecting pairs of microbands via an ammeter (Model 6517B Electrometer, Keithley Instruments, Inc., Cleveland, OH). As previously mentioned, the split BPE design more closely mimicked the electrode area of a continuous BPE,[1−3] and therefore, it provided a point of comparison for the current measured using the microband BPEs. Data were processed using LabView software (National Instruments, Austin, TX). Simultaneous measurement of the total current through the microfluidic channel was achieved by monitoring the voltage drop across a 523 kΩ resistor in series with the microchannel. These measurements were made with a hand-held, digital multimeter equipped with PC-Link software (VA18B, Sinometer Instruments, ShenZhen, China).

Electric Field Profile Measurements. The electric field profile within a buffer-filled channel was measured as follows. First, a pair of microbands having an appropriate spacing was connected to form a BPE. Second, the Keithley electrometer (set in voltage measurement mode) was connected between the pair of microband electrodes adjacent to the BPE on the anodic side of the channel. Third, 35.0 V was applied across the microchannel via the driving electrodes. When the measured voltage attained a constant value (~200 s), ΔE for all other neighboring pairs of microbands was measured. The voltage between the original pair of microbands was periodically remeasured to ensure that its value remained constant during the experiment. Finally, this process was repeated several times using different pairs of microbands to define the BPE.

RESULTS AND DISCUSSION

Concentration Enrichment. Concentration enrichment is initiated by connecting two of the band electrodes in the microarray with a jumper wire and then applying a suitable potential (E_{tot}) between the two driving electrodes (Figure 1b). In this configuration, the connected pair of microband electrodes behaves as a single, discontinuous BPE. When E_{tot} attains a sufficiently high value, water electrolysis is induced at the ends of the BPE. The resulting anodic and cathodic reactions are given in eqs 1 and 2, respectively.

$$2H_2O - 4e^- \rightarrow O_2 + 4H^+ \qquad E^\circ = 0.40\ V \qquad (1)$$

$$2H_2O + 2e^- \rightarrow H_2 + 2OH^- \qquad E^\circ = -0.83\ V \qquad (2)$$

$$TRISH^+ + OH^- \rightarrow TRIS + H_2O \qquad (3)$$

A consequence of these processes is the neutralization of the buffer cation ($TRISH^+$) by OH^- generated at the cathode end of the BPE (eq 3). This homogeneous reaction results in a region of low conductivity that starts at the cathode end of the BPE (right side, Figure 1) and extends into the anodic compartment of the microchannel. An extended electric field gradient results, which provides a region for analyte focusing.[1,2] Note that enrichment is not due to a pH gradient, because the presence of the buffer resists dramatic changes in pH.

The fluorescence micrograph shown in Figure 2a demonstrates concentration enrichment of $BODIPY^{2-}$ using a continuous BPE 800 s after the driving voltage (E_{tot} = 35.0 V) was applied. This result is consistent with our previous reports.[1,2] Comparable behavior is observed at an array of microband electrodes (Figure 2b). In this experiment, electrodes 5 and 11 were externally connected, as shown schematically in Figure 1b, to form the BPE. The approximate potential drop across the BPE, ΔE_{elec}, is given by eq 4.

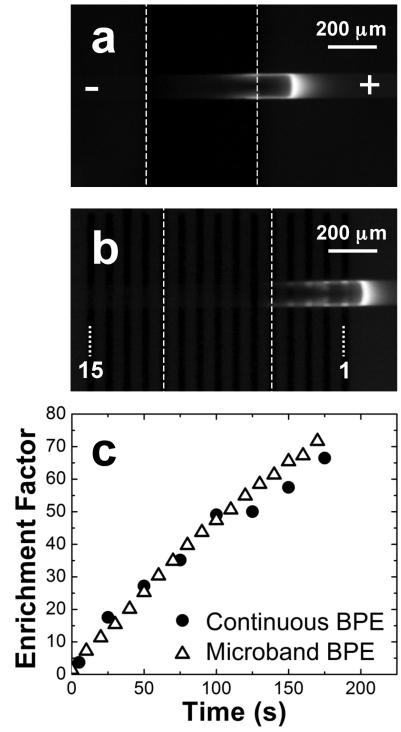

Figure 2. Fluorescence micrographs demonstrating concentration enrichment of BODIPY disulfonate after enriching for (a) 800 s at a continuous BPE of total length 500 μm and (b) 160 s at a microband array consisting of 40 μm lines and spaces in which electrodes 5 and 11 are connected to form a BPE of ~520 μm total length. The images are top views, and the dashed white lines indicate the location of the BPE. Initial concentration of $BODIPY^{2-}$ is 0.1 μM in 5.0 mM TRIS buffer (pH 8.0); E_{tot} = 35.0 V. (c) Comparison of the enrichment factor for $BODIPY^{2-}$ at the microband array BPE and a continuous BPE. Enrichment factor is determined by dividing the maximum $BODIPY^{2-}$ concentration attained by the initial concentration.

$$\Delta E_{elec} = \frac{E_{tot} \cdot l_{elec}}{l_{channel}} \qquad (4)$$

Here, $l_{channel}$ is the length of the channel (6 mm), l_{elec} is the effective length of the bipolar electrode (0.52 mm), and E_{tot} = 35.0 V. For this experiment, ΔE_{elec} = 3.0 V. Note that this simple analysis assumes all of E_{tot} is dropped within the channel and that the potential profile across the channel is linear. However, we are mindful that this is just a useful approximation and that the real situation is slightly more complex.[45] For example, a fraction of E_{tot} is dropped at the driving electrodes.[46] Nevertheless, as will be explicitly demonstrated later, E_{tot} = 35.0 V is sufficient to drive the electrochemical reactions

(45) Mavré, F.; Chow, K.-F.; Sheridan, E.; Chang, B.-Y.; Crooks, J. A.; Crooks, R. M. *Anal. Chem.* **2009**, *81*, 6218–6225.

(46) Bard, A. J.; Faulkner, L. R. *Electrochemical methods: fundamentals and applications*, 2nd ed.; John Wiley & Sons: Hoboken, NJ, 2001; p 833.

represented by eqs 1 and 2, even though they do not occur at their thermodynamic potentials. This results in the extended field gradient in solution that is required for analyte concentration. Indeed, $BODIPY^{2-}$ concentrates ~350 μm to the right of electrode 5, thereby exhibiting behavior very similar to that observed at the continuous BPE (compare Figure 2a,b).

Figure 2c is a plot of measured enrichment factor versus time for both the continuous and microband BPEs. The important point is that the time course of the enrichment is essentially independent of the electrode design. Specifically, both configurations result in an enrichment factor of ~70 after 180 s. The correspondence between the behavior of the two types of electrodes highlights the suitability of the microband array as a tool for developing a better understanding of continuous BPEs.

BPE Current Measurement. An important parameter that affects bipolar electrode focusing is the magnitude of the current passing through the BPE. Here, we compare this faradaic current for the split (Figure 1e) and microband (Figure 1c) BPE designs and correlate these values to the onset of concentration enrichment. For these experiments, the two halves of the BPEs were connected in series with an ammeter external to the channel. We have previously shown that the presence of the ammeter does not significantly affect the current passing through the electrode.[45] The steady-state current (i_{BPE}) was measured in split and microband BPEs having similar total lengths (l_{elec} = 500 and 520 μm, respectively) during focusing of 0.1 μM $BODIPY^{2-}$ in 5 mM TRIS buffer with E_{tot} = 35.0 V. For the split BPE, i_{BPE} = 271 nA and i_{tot} = 328 nA. For the microband array, i_{BPE} = 225 nA and i_{tot} = 285 nA. Importantly, ~80% of the total channel current is diverted through the BPE regardless of design. As discussed below, it is this high value of i_{BPE}/i_{tot} that is responsible for the modulation of the local electric field and hence focusing of the tracer.

This relationship between the magnitude of the faradaic current and the onset of concentration enrichment is clearly observed at the very start of an experiment in a newly prepared microfluidic device. Under these conditions, i_{BPE} is low when E_{tot} is first applied (i_{BPE}/i_{tot} < 20%). However, after a few minutes, i_{BPE} increases rather suddenly (i_{BPE}/i_{tot} > 80%). Importantly, this increase is accompanied by the onset of enrichment.

Because of the relationship between faradaic processes at the BPE and the onset of enrichment, it is important that E_{tot} be high enough to drive faradaic production of OH^- at the BPE cathode and hence neutralization of $TRISH^+$ (eqs 2 and 3). Accordingly, the split BPE configuration was used to measure the fraction of the total current that is carried by the BPE (i_{BPE}/i_{tot}) as a function of E_{tot} (Figure 3). Simultaneous measurement of i_{BPE} and i_{tot} is achieved by connecting the two halves of the BPE through an ammeter and monitoring the voltage drop across a resistor in series with the microchannel (inset of Figure 3). Measurements of i_{BPE}/i_{tot} at each value of E_{tot} were made at t = 1500 s which, in all cases, is several hundred seconds after this ratio achieved a constant value. The results in Figure 3 show that a threshold value of the driving voltage of between E_{tot} = 20.0 and 25.0 V must be reached before a significant fraction of channel current is diverted through the BPE. Using eq 4, these values of E_{tot} correlate to ΔE_{elec} = ~1.7 and ~2.0 V, respectively, which is consistent with our earlier contention that electrolysis of water

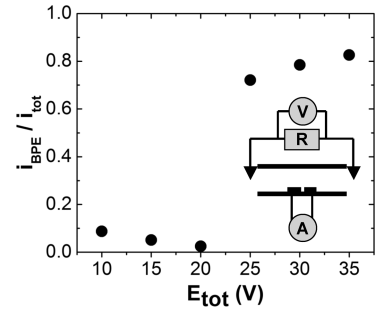

Figure 3. Steady-state ratio of BPE current (i_{BPE}) to total current (i_{tot}) obtained for several values of E_{tot} with 5.0 mM TRIS (pH 8.0) and no $BODIPY^{2-}$ present in the channel. Currents were recorded 1500 s after application of E_{tot}. Measurements were made with a split BPE configured as represented schematically in the inset.

is responsible for i_{BPE}. This threshold provides a lower bound for the selection of E_{tot} while the upper bound is defined by the onset of O_2 and H_2 bubble formation at the BPE (eqs 1 and 2). The formation of bubbles is dependent not only on E_{tot} (and the associated heterogeneous reaction rate) but also on the rate of diffusive and convective transport, which prevent accumulation of the gases. A larger accessible range of E_{tot} allows greater breadth of control during the optimization of electric field characteristics.

Microchannel Electric Field Profile Measurements. The shape of the electric field gradient in the microchannel determines the extent and location of concentration enrichment. In this section, we show how the microband array can be used to map the field gradient, and then we compare the experimental results to numerical simulations. These experiments were carried out in several steps. First, the microchannel was filled with 5 mM TRIS buffer (no $BODIPY^{2-}$) with an excess (8 μL, which corresponds to a 0.2 mm height difference) in the cathodic reservoir. Although an excess volume in the anodic reservoir tends to prevent concentration enrichment, excess volume in the cathodic reservoir is found to stabilize both enrichment and the observed electric field profile. This might be due to a slight counterflow opposing the electroosmotic flow. Second, one pair of electrodes was connected via an external jumper wire to yield a bipolar electrode. Third, E_{tot} = 35.0 V was applied to initiate the formation of the electric field gradient used for focusing. Simultaneously, the voltage drop between the pair of electrodes adjacent to the BPE cathode was monitored until it reached steady state (~200 s). Fourth, the potential between the remaining electrode pairs (except those acting as the BPE) was sequentially measured to map out the electric field. Because the sensing microband electrodes are connected by a high-impedance voltmeter, they are not able to function as BPEs.

Figure 4a shows the steady-state electric field profile measured under enrichment conditions but in the absence of the $BODIPY^{2-}$ tracer. Measured voltages are divided by the center-to-center distance between microbands to obtain the average field strength for each 80 μm segment. The results (and error bars) shown in Figure 4a represent data from several sets of measurements on two separate devices. Each set of measurements was taken using a different pair of electrodes to form the BPE (1 and 7, 5 and 11, 6 and 12, or 9 and 15). The arrows in this figure

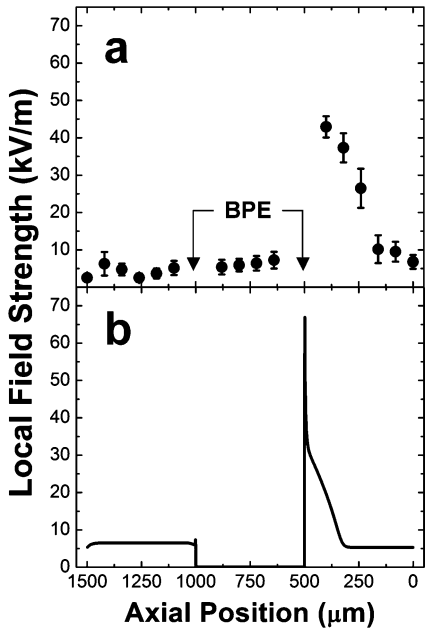

Figure 4. (a) Steady-state electric field strength averaged over 80 μm distances between neighboring microband electrodes. The data are averaged over two separate devices. In each case, several maps of the electric field were obtained by the use of a different pair of microbands to define the BPE during each set of measurements. No BODIPY^{2-}, 5.0 mM TRIS, $E_{tot} = 35.0$ V. (b) Simulated axial electric field at $y = 3.5$ μm at $t = 60$ s after application of driving voltage (at 5.83 kV/m). The 2D simulated geometry is 1500 μm long with a 3 μm tall BPE from $x = 500$ to 1000 μm. The zeta potential on the channel walls is assumed to be −85 mV. The initial condition is a uniform distribution of 5.0 mM TRIS.

indicate the location of the microbands comprising the BPE. The results indicate that there is a marked increase in the field strength to the right of the BPE cathode. This increase is due to the neutralization of TRISH$^+$ by OH$^-$ and the formation of a corresponding low conductivity zone. The extended field gradient is at a maximum of ~40 kV/m at the BPE edge and gradually decreases to 10 kV/m at a distance of 400 μm from the electrode. The field strength continues to decrease at farther distances but at a lower rate. It is also apparent that the electric field between the outer edges of the BPE is essentially unchanged. Finally, the electric field in the cathodic compartment, to the left of the BPE, does not reveal any defining features but rather appears to be somewhat suppressed (4.0 kV/m average).

These findings compare favorably to numerical simulations with a continuous BPE. Complete details regarding the conditions used for the simulations have been provided previously.[2] Briefly, a 1500 μm segment of the microchannel with the 500 μm BPE at the center ($x = 500$ to 1000 μm) was approximated by a two-dimensional model (Figure 4b). The time-dependent redistribution of ions in solution was modeled taking into consideration convection and diffusion, buffer reactions, faradaic processes, and the effects of the applied electric field (5.8 kV/m) including electromigration of ions and electroosmotic flow. The initial condition is a uniform distribution of 5.0 mM TRIS buffer. Figure 4b shows the resulting electric field profile at $t = 60$ s for a cross section 0.5 μm above the BPE surface. The magnitude of the electric field is zero over the interior of the BPE and close to 6.5 kV/m in the cathodic compartment. Most significantly, the results reveal the extended field gradient required for bipolar electrode focusing in the anodic compartment with a maximum field strength located at the edge of the BPE cathode and decreasing to the right.

There are two main differences between the simulated and experimental results. First, the simulation leads to a somewhat smaller magnitude and extension of the electric field gradient. This difference is most likely due to the ambiguity involved in selecting diffusion coefficients and reaction rates from the literature for simulation parameters. Taking this into consideration, along with the sensitivity of the system to small changes in conditions, the agreement of the resulting electric field gradient to within 30−40% of the measured magnitude is remarkably good. Second, in the simulation, the electric field in the region directly above the BPE is near zero. The absence of complete suppression of the electric field over the BPE in the experimental results is unexpected considering the high magnitude of i_{BPE}/i_{tot}. When ~80% of the ionic current is diverted through the BPE, it is expected that the electric field in solution over the BPE will be ~80% weaker due to a simple Ohm's Law argument. However, this argument assumes that the solution resistance in the region over the BPE remains constant. If there is extensive depletion of ions above the BPE, increased solution resistance will proportionally augment the electric field in that region. While the simulations do account for some ion depletion in solution over the BPE, our electric field measurements indicate further depletion.

Unidirectional Band Motion. Microband arrays permit positional control of the focused tracer band within the microchannel. In this section, we describe the controlled transport of the enriched tracer zone between two locations, depending on which microbands are connected. We used a microband array having 20 μm lines and 80 μm spaces for these experiments. The wider spaces in this version of the microarray provide a clearer view of the focused analyte movement than the 40 μm spaces used for the just-described field profiling measurements. Positional control of the enriched band was carried out as follows. First, 30.0 μL of 0.1 μM BODIPY^{2-} and 5.0 mM TRIS solution was added to each reservoir. Second, $E_{tot} = 30.0$ V was applied across the microchannel ($\Delta E_{elec} = 3.6$ V). Third, to generate band movement, a switch was used to alternately connect two separate pairs of electrodes (1 with 8 and 7 with 14). Switching between the two configurations results in analyte focusing just to the right of either electrode 1 or electrode 7 (Figure 5a,b, respectively). These are referred to hereafter as positions 1 and 7. These fluorescent micrographs demonstrate the formation of a tracer band after switching to each position for 50 and 25 s, respectively.

We observe that, upon switching from position 1 to position 7, the band is transferred from right to left and stopped at position 7. However, upon switching back to position 1, the original band continues in the direction of the EOF, out of the channel, while a new band begins to form at position 1. Movie S1 (Supporting Information), which plays at a frame rate 10× real time, demonstrates this phenomenon when the switch is triggered at 25 s and, thereafter, at 50 s intervals. The mechanism for band relocation from 1 to 7 is explained by the redevelopment of the extended

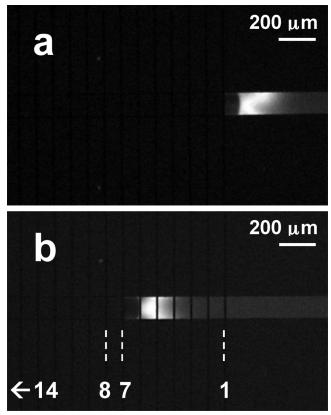

Figure 5. Fluorescence micrographs from Movie S1 (see the Supporting Information) showing the concentrated band of $BODIPY^{2-}$ at two locations. The position is controlled by connecting different pairs of microbands to form the BPE. Here, the BPEs were formed by connecting electrodes (a) 1 and 8 or (b) 7 and 14. The bands shown in (a) and (b) were enriched for 50 and 25 s, respectively.

field gradient "downstream" (left) of the initial band location. The inability of the band to return from left to right is a consequence of reformation of the extended field gradient "upstream" in an area inaccessible to the band. This is strong evidence of the relative magnitudes of the electrophoretic and electroosmotic velocities in each segment of the microchannel. This behavior also demonstrates that the electric field gradient forms very rapidly. After switching from position 1 to 7, the new field gradient must form at position 7 within ~2 s in order to "catch" the concentrated tracer band. Contrast this time interval with that discussed earlier for the very first enrichment experiment carried out using a freshly prepared microfluidic device (a few minutes).

SUMMARY AND CONCLUSIONS

We have demonstrated bipolar electrode focusing at continuous and discontinuous BPEs in a microfluidic device. Three discontinuous designs, two microband arrays and a split BPE, provide an approximation of the continuous BPE system we have reported previously. These new designs provide important insights into the focusing process. Measurement of the BPE current reveals an onset of electrolysis above $E_{tot} = 20.0$ V ($\Delta E_{elec} \approx 1.7$ V), and confirms that these faradaic reactions must proceed at an appreciable rate in order for enrichment to occur. Further investigation by mapping of the electric field in the vicinity of the BPE provides support for previously reported simulation results, highlighting in particular the development of an extended field gradient in the anodic compartment.

Experiments and simulations demonstrate a 5- to 7-fold increase in the electric field adjacent to the BPE cathode relative to the strength of the average applied electric field. Finally, a novel means of analyte band transport has been developed that takes advantage of the flexibility of the microband array design. This approach might prove useful for extraction and subsequent delivery of discrete, concentrated packets of analytes to remote on-chip processing modules without the need for additional hardware. More refined, bidirectional control over analyte band location may soon be achieved using a combination of microband arrays and pressure driven flow.

In our ongoing research, we aim to use microband arrays for the simultaneous concentration, separation, and electrochemical detection of analytes by employing additional bands for amperometric detection. We also anticipate that further electric field mapping studies will shed light on the effect of experimental conditions on the shape of the electric field and focusing conditions.

ACKNOWLEDGMENT

We gratefully acknowledge support from the Chemical Sciences, Geosciences, and Biosciences Division, Office of Basic Energy Sciences, Office of Science, U.S. Department of Energy (Contract No. DE-FG02-06ER15758). We also thank the Robert A. Welch Foundation (Grant F-0032). Simulations were run at the "Leibniz-Rechenzentrum der Bayerischen Akademie der Wissenschaften" (Garching, Germany), supported by project HLRB pr26wo. This material is based in part upon work supported under a National Science Foundation Graduate Research Fellowship to R.K.P.

SUPPORTING INFORMATION AVAILABLE

Movie S1 (.avi) demonstrates unidirectional motion of a concentrated band. Details regarding the movie are provided in the text. This material is available free of charge via the Internet at http://pubs.acs.org.

Received for review August 24, 2009. Accepted October 30, 2009.

AC901913R